Astronomy & Astrophysics manuscript no. FREDs-v1.3
February 5, 2020

LETTER TO THE EDITOR

Searching for galactic sources in the *Swift* GRB catalog

Statistical analyses of the angular distributions of FREDs

J.C. Tello[1], A.J. Castro-Tirado[1], J. Gorosabel[1], D. Pérez-Ramírez[2], S. Guziy[3], R. Sánchez-Ramírez[1], M. Jelínek[1], P. Veres[4,5], and Z. Bagoly[4]

[1] Instituto de Astrofísica de Andalucía (I.A.A.-C.S.I.C.), Spain
[2] Universidad de Jaén, Spain
[3] Nikolaev National University, Ukraine
[4] Eötvös University, Budapest
[5] Bolyai Military University, Budapest

Preprint online version: February 5, 2020

ABSTRACT

Context. Since the early 1990s, gamma ray bursts (GRB) have been accepted to be of extra-Galactic origin because of the isotropic distribution observed by BATSE and the redshifts observed via absorption line spectroscopy. Nevertheless, upon closer examination at least one case turned out to be of Galactic origin. This particular event presented a fast rise, exponential decay (FRED) structure, which leads us to believe that other FRED sources might also be Galactic.
Aims. This study was set out to estimate the most probable degree of contamination by Galactic sources that certain samples of FREDs have.
Methods. To quantify the degree of anisotropy, the average dipolar and quadripolar moments of each sample of GRBs with respect to the Galactic plane were calculated. This was then compared to the probability distribution of simulated samples comprising a combination of isotropically generated sources and Galactic sources.
Results. We observe that the dipolar and quadripolar moments of the selected subsamples of FREDs are found more than two standard deviations outside those of random isotropically generated samples. The most probable degree of contamination by Galactic sources for the FRED GRBs of the *Swift* catalog detected until February 2011 that do not have a known redshift is about 21 out of 77 sources, which represents roughly 27%. Furthermore, we observe that by removing from this sample those bursts that have any type of indirect redshift indicator and multiple peaks, the most probable contamination increases to 34% (17 out of 49 sources).
Conclusions. It is probable that a high degree of contamination by Galactic sources occurs among the single-peak FREDs observed by *Swift*. Accordingly we encourage additional studies on these type of events to determine the nature of what could be an exotic type of Galactic source.

Key words. (stars:) Gamma-ray burst: general – stars: magnetars – methods: statistical

1. Introduction

Gamma ray bursts (GRBs) are the most energetic explosions known in the Universe, second only to the Big Bang. Discovered in the 1960s, they were widely believed to originate in the Milky Way because of their relatively high flux of photons, which needs an unprecedented emission mechanism to account for this high energy output. It was not until 1997 when the first measurement of redshift was performed on a GRB afterglow that the cosmological nature of these objects was asserted without doubt (Metzger et al. 1997).

The GRB afterglows fade within a few hours, and as a consequence, the redshift of most GRBs are unknown. In the past several studies have been carried out to indirectly determine the Galactic or extra-Galactic nature of the bursts by analyzing their spatial distribution in the sky (Balazs et al. 1998; Mazets et al. 1981; Meegan et al. 1992), and historically it served as a strong argument against the Galactic origin of GRBs (Paciesas et al. 1999). This technique has also been used to suggest a more local nature of long-lag bursts by showing that they may be related to the super-Galactic structure (Foley et al. 2008; Norris 2002).

The observed light curve of each GRB varies from burst to burst, particularly during in the prompt phase when the gamma ray emission is emitted, where one or multiple peaks with a variety of shapes are observed. However, some of them present a fast rise and exponential decay (FRED hereafter) behavior. These have been correlated with other properties of the bursts (Bhat et al. 1994), suggesting that they may be of a different nature than other GRBs.

There has been at least one reported GRB that upon closer examination has resulted to be a phenomenon from within the Milky Way (Castro-Tirado et al. 2008; Stefanescu et al. 2008). This source displayed a FRED structure, which leads us to believe that there could be others like it.

We aim to estimate the most probable degree of contamination by Galactic sources that certain samples of FREDs have. We have organized the paper as follows: in Section 2 we establish the selection criteria of the studied samples. Section 3 describes the methodology used for quantifying the anisotropy and determining the probability of observing these values for both extra-Galactic and Galactic sources while taking into account the exposure of *Swift*. We discuss the results from our analysis in Section 4 and give our main conclusions in Section 5.

2. Sample selection

To achieve a homogeneous distribution, only *Swift*-detected GRBs were taken into account. From the catalog of 596 GRBs detected by *Swift* before March 2011, 111 GRBs were selected because they had a FRED structure reported in a GCN. Using the information available in peer-reviewed papers[1] and other GCN circulars related to the 111 FRED GRBs, the following subsamples were selected: [2]

- **Sample 1:** All 111 FREDs detected by *Swift* until February 2011.
- **Sample 2:** 77 FREDs without any measured redshift.
- **Sample 3:** 71 FREDs without stated high-redshift criteria.
- **Sample 4:** 59 FREDs without any type of indirect redshift indication.
- **Sample 5:** 49 FREDs without any redshift indications or multiple peaks.

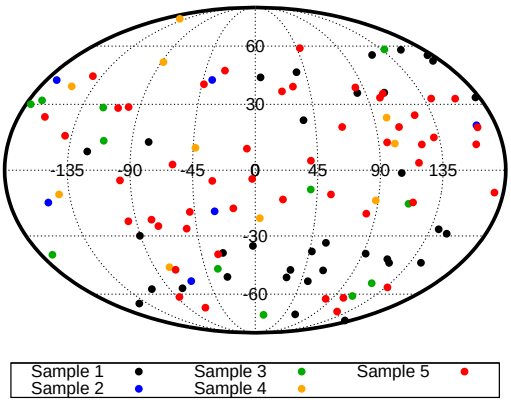

Fig. 1. Sources in each one of the samples.To avoid redundancy, only the sources not present in the subsequent samples were included.

It is important to note that only sample 5 included solely those bursts that consisted of one pure FRED peak.

3. Anisotropy quantification

It has been proven (Hartmann & Epstein 1989) that the mean dipolar and quadripolar moments of the Galactic coordinates ($cosb$ and sin^2b, where b is the Galactic latitude) are good tools to quantify the isotropy with respect to the Galactic plane (Castro Tirado 1994). The degree of isotropy of each sample was calculated using the coordinates available from the gamma-ray burst coordinate network (GCN) circulars for each burst. The results are shown in Table 1.

3.1. Exposure map

Owing to the nature of its instruments, orbit, and mission, *Swift*'s pointing toward the sky is not homogeneous. It is of particular relevance to note that there has been less integrated exposure time toward the Milky Way's disk than toward the Galactic poles. This fact would represent a bias for the nature of the study

[1] Only two peer-reviewed papers were relevant for the sample selection (Clemens et al. 2011; Perley et al. 2009)

[2] For a list of specific selected bursts see Appendix A

Sample	$< cosb >$	$< sin^2b >$
#1	0.7883	0.3397
#2	0.8221	0.2860
#3	0.8184	0.2909
#4	0.8344	0.2673
#5	0.8397	0.2622

Table 1. Dipolar and quadripolar moments of the samples as a quantitative measurement of the degree of isotropy in the samples.

carried out for this publication if left unaccounted, therefore we created a map by integrating the exposure mask function for the BAT instrument, multiplied by the exposure times of all observations carried out between April 16, 2005 and February 1, 2011, taking into account the pointing and rotation of the BAT instrument[3].

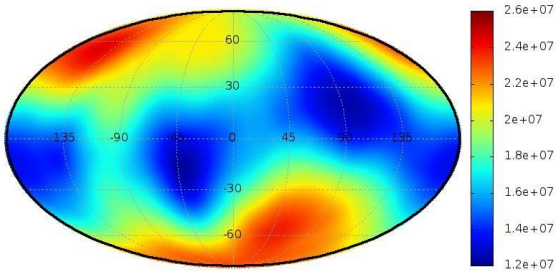

Fig. 2. Swift exposure map in Galactic coordinates derived for this study. Colors represent the exposure time (in seconds).

3.2. Monte Carlo simulations

Monte Carlo simulations were carried out to determine the probability mass function (PMF) of the average dipolar and quadripolar moments of random GRB distributions. Therefore random coordinates were generated, taking care that they had a homogeneous distribution on an spherical surface.

These random points were then used to determine the PMF of the dipolar and quadripolar moments of random sources in the sky to determine by how much the observed samples' values deviated from those of a completely isotropically generated sample. To do this we generated an equal number of random points to that of each sample, recording the value of the mean dipolar and quadripolar moment and iterating a statistically significant number of times 10^6 – 10^9 iterations. The histogram of the recorded values was then used to determine the values for standard deviations ($\sigma, 2\sigma, 3\sigma$).

3.3. Metropolis-Hastings algorithm

To account for the anisotropy of *Swift*'s exposure of the night sky, it was necessary to factor in the probability that a particular random source was detected by *Swift*. We used the Metropolis-Hastings algorithm for this, which can be summarized in three steps:

1. Create a random source (set of coordinates).

[3] The method used to derive the exposure map is the same as the one detailed in Veres *et al.*, 2010

Sample	Dipolar	Quadripolar
#1	78.24	13.26
#2	97.91	0.59
#3	96.72	1.03
#4	98.52	0.44
#5	97.83	0.39

Table 2. Percentile of the values observed for the dipolar and quadripolar moments of each sample.

2. Create a random number with a range equal to the values of the map or mask.
3. Compare the value of the map at those coordinates to the random number.
4. If the value of the point on the map exceeds the random number, then the random source is included in the sample for further analysis. Otherwise a new random source is created and the process is repeated until the correct amount of sources is obtained.

This will effectively generate random sources that are more likely to appear where the exposure is higher. This method was tested by generating a statistically significant number of random sources and checking that the resulting image was one proportional to the weighting mask well within normal statistical fluctuations.

3.4. Contamination by Galactic sources

Considering that i) the density of matter of the Milky Way is roughly correlated with the amount of interstellar dust, and by consequence so is the amount of stellar sources, and ii) the transparency of gamma-rays to interstellar dust, we used maps of dust IR emission (Schlegel et al. 1998) as a weighting mask for the Metropolis-Hastings algorithm to generate random Galactic sources.

The isotropically generated samples were contaminated by increasing the number of Galactically generated random sources (N) to observe how this affected the PMF of their dipolar and quadripolar moment. We considered all possible combinations for the number of GRBs in the different samples and took into account the *Swift* exposure map for each generated source.

4. Results

The Monte Carlo simulations of the isotropically generated random samples (weighted by the *Swift* exposure map) showed that the dipolar and quadripolar moments from the real samples consistently deviated from the average, as is shown in Figure 3.

Table 2 lists the percentile of the population in which each sample is located. Considering that by definition, one standard deviation will be between the 15.87th and the 84.13th percentiles, two standard deviations between 2.28th and 97.72th and three deviations between 0.13th and 99.87th, we observe that with the exception of the first sample, all samples have dipolar and quadripolar moments located outside two standard deviations.

The probability distribution of samples that contained both isotropically and Galactically generated sources allowed us to compare how the contamination by Galactic sources affected the likelihood of obtaining certain momentum values, for example see figure 4. This technique is similar to the one used in the past for studying the degree of contamination by

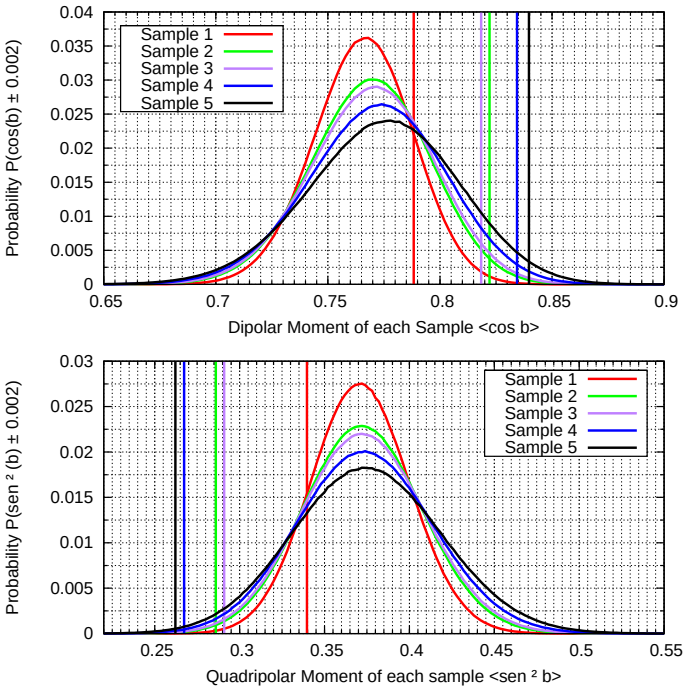

Fig. 3. Dipolar (**top**) and quadripolar (**bottom**) moment PMFs for samples of isotropically generated sources weighted by *Swift*'s exposure map for each sample size, and the observed values for each sample (vertical lines).

Sample #:	1	2	3	4	5
Dipolar:	13	20	17	18	16
Dipolar %:	11.71%	25.97%	23.94%	30.51%	32.65%
Quadripolar:	12	22	20	21	18
Quad. %:	10.81%	28.57%	28.17%	35.59%	36.73%

Table 3. Amount of Galactic sources that yield a higher probability to obtain the observed dipolar and quadripolar moments and the percentage of the sample size they imply.

Galactic repeater gamma-ray sources present in two GRB catalogs (Gorosabel et al. 1998).

By observing the probability of the observed values in each one of the curves that resulted from the simulations, we determined the relative probability that each one of those combinations of isotropically and Galactically generated sources would yield the observed momentums. Figure 5 shows the probability as a function of the amount of Galactic sources introduced in each sample.

5. Conclusions

With the exception of the first sample, all observed samples show dipolar and quadripolar moments outside two standard deviations from the mean of an isotropically generated distribution. Although this result is not conclusive, there is a high probability that the samples are not of a purely Extra-Galactic nature.

The probability of obtaining the dipolar and quadripolar moments that are measured in the samples is much higher when including a significant amount of Galactic sources than it is for only isotropically generated sources.

As shown in Table 3, if we consider the amount of contamination that yields the highest probability of obtaining the observed values, the amount of Galactic sources that are probably

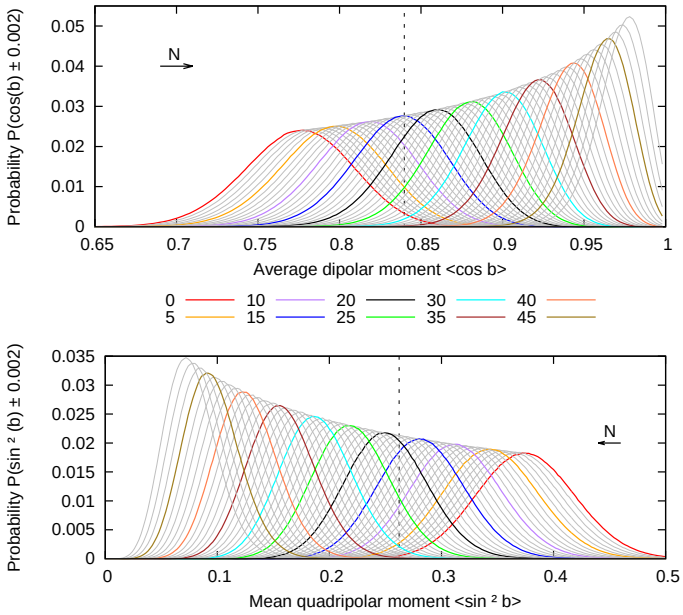

Fig. 4. Example of dipolar (**top**) and quadripolar (**bottom**) moment probability distributions for samples of 49 randomly generated sources with an increasing number (**N**) of those sources being of Galactic origin, and the observed value for sample #5 (dashed vertical line). Each line has a different amount of Galactic sources, starting with N=0 (red), and only every fifth line was colored for easier reading.

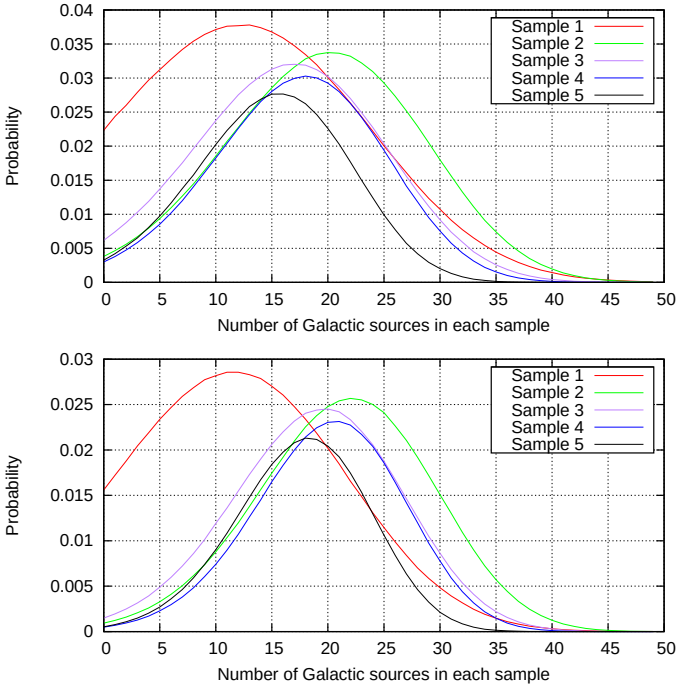

Fig. 5. Relative probability of obtaining the dipolar (**top**) and quadripolar (**bottom**) moments ±0.002 measured for our samples.

contaminating the *Swift* GRB catalog is between 16 and 22. This value represents approximately 3% of the catalog used for this study.

Sample 5 has been narrowed down so that it is likely that one out of every three is in fact a Galactic source, accordingly it is of great interest to study these sources in more detail to determine if there are other indications that they are not GRBs.

The high Galactic extinction discourages optical ground-based spectroscopy of most low Galactic latitude GRBs. We showed that a large part of those abandoned follow-ups could reveal a missing population of Galactic events. We encourage ground observers to follow-up those events, since it might lead to the discovery of unknown high-energy phenomena in our Galaxy.

Acknowledgements. We have made use of J. Greiner's GRB Table (http://www.mpe.mpg.de/~jcg/grbgen.html)

This research has been partially supported by the Spanish Ministry of Economy and Competitivity under the programmes AYA2011- 24780/ESP, AYA2009-14000-C03-01/ESP, and AYA2012-39362-C02-02 and OTKA grant K077795.

References

Balazs, L. G., Meszaros, A., & Horvath, I. 1998, A&A, 339, 1
Bhat, P. N., Fishman, G. J., Meegan, C. A., et al. 1994, ApJ, 426, 604
Castro Tirado, A. J. 1994, The WATCH experiment: 1000 days observing the X-ray universe.
Castro-Tirado, A. J., de Ugarte Postigo, A., Gorosabel, J., et al. 2008, Nature, 455, 506
Clemens, C., Greiner, J., Krühler, T., et al. 2011, A&A, 529, A110
Foley, S., McGlynn, S., Hanlon, L., McBreen, S., & McBreen, B. 2008, A&A, 484, 143
Gorosabel, J., Castro-Tirado, A. J., Brandt, S., & Lund, N. 1998, A&A, 336, 57
Hartmann, D. & Epstein, R. I. 1989, ApJ, 346, 960
Mazets, E. P., Golenetskii, S. V., Ilinskii, V. N., et al. 1981, Ap&SS, 80, 3
Meegan, C. A., Fishman, G. J., Wilson, R. B., et al. 1992, Nature, 355, 143
Metzger, M. R., Djorgovski, S. G., Kulkarni, S. R., et al. 1997, Nature, 387, 878
Norris, J. P. 2002, ApJ, 579, 386
Paciesas, W. S., Meegan, C. A., Pendleton, G. N., et al. 1999, ApJS, 122, 465
Perley, D. A., Cenko, S. B., Bloom, J. S., et al. 2009, AJ, 138, 1690
Schlegel, D. J., Finkbeiner, D. P., & Davis, M. 1998, ApJ, 500, 525
Stefanescu, A., Kanbach, G., Słowikowska, A., et al. 2008, Nature, 455, 503
Veres, P., Bagoly, Z., Horváth, I., et al. 2010, in American Institute of Physics Conference Series, Vol. 1279, American Institute of Physics Conference Series, ed. N. Kawai & S. Nagataki, 457–459

This appendix specifies which bursts are included in each one of the five samples used in this study. To facilitate its reading each column was named in reference to the discriminating parameter for each subsample. That is:

- **Sample 1:** All 111 FREDs detected by *Swift* before March 2011.
- **Sample 2:** 77 FREDs without any measured redshift different from zero
- **Sample 3:** 71 FREDs without any claimed high redshift criteria
- **Sample 4:** 59 FREDs without any type of indirect redshift indication
- **Sample 5:** 49 FREDs without any redshift indications or multiple peaks

With the exception of the first column and where noted otherwise, each number refers to the GCN circular.

GRB#	F.R.E.D.	Redshift	”High-z”	Any z	Peaks
050315	3094	3101	-	-	-
050319	3117	3135	-	-	-
050406	3183	none	none	none	none
050421	3305	none	none	none	none
050603	3512	3520	-	-	-
050713B	3600	none	none	none	none
050717	3633	none	none	none	3633
050721	3661	none	none	none	none
050801	3725	none	none	none	none
050826	3888	none	5982	-	-
051016	4102	4391	-	-	-
051021B	4126	none	none	none	none
051111	4260	4255	-	-	-
051117A	4289	none	none	none	none
051227	4401	none	none	4399	-
060110	4463	none	none	none	none
060213	4762	none	none	4769	-
060403	4945	none	none	none	none
060515	5141	none	none	none	none
060522	5153	5155	-	-	-
060526	5163	5164	-	-	-
060604	5212	5218	-	-	-
060605	5221	5223	-	-	-
060607	5242	5237	-	-	-
060707	5285	5298	-	-	-
060719	5349	none	none	none	none
060904B	5520	none	none	5507	-
060912	5558	5565	-	-	-
060919	5578	none	none	none	none
060926	5621	5626	-	-	-
061102	5777	none	none	none	none
061110A	5802	5812	-	-	-
061202	5887	none	none	none	none
061210	5905	none	none	none	none
061222A	5964	none	none	Paper:(Perley et al. 2009)	-
070208	6081	6080	-	-	-
070219	6109	none	none	none	none
070318	6210	6213	-	-	-
070326	6653	none	none	none	none
070330	6237	none	6238	-	-
070509	6394	none	none	none	none
070518	6415	none	none	none	none
070520B	6438	none	none	none	none
070531	6475	none	none	none	none
070612	6509	none	none	6510	-
070808	6718	none	none	6720	-
070810B	6753	none	none	6756	-
070917	6791	none	none	6799	-
071010B	6871	6884	-	-	-
071028	7013	none	none	none	none

GRB#	F.R.E.D.	Redshift	”High-z”	Any z	Peaks
071028B	7019	none	none	Paper:(Clemens et al. 2011)	-
071112C	7081	7070	-	-	-
071117	7098	none	none	7108	-
080303	7351	none	none	none	none
080307	7362	none	7362	-	-
080319C	7442	7468	-	-	-
080320	7473	none	none	7474	-
080325	7531	none	none	none	none
080413B	7606	7598	-	-	-
080430	7647	7647	-	-	-
080503	7673	none	none	none	7673
080517	7748	none	7748	-	-
080523	7772	none	7772	-	-
080613B	7876	none	none	none	7873
080701A	7913	none	none	none	none
080702B	7924	none	none	none	none
080707	7952	7948	-	-	-
080710	7969	7962	-	-	-
080714	7979	none	none	none	none
080727B	8030	none	8033	-	-
080805	8059	8060	-	-	-
080903	8176	none	none	none	none
080915B	8234	none	none	none	none
080916A	8243	8254	-	-	-
081104	8479	none	none	none	none
081121	8537	8542	-	-	-
090129	8861	none	none	none	none
090401B	9068	none	none	none	9066
090518	9393	none	none	none	none
090520	9417	none	none	none	none
090530	9443	none	none	none	9443
090726	9706	9712	-	-	-
090727	9724	none	none	none	9724
090904A	9888	none	none	none	none
091018	10034	10038	-	-	-
091024	10072	10065	-	-	-
091026	10081	none	none	none	none
091208A	10253	none	none	none	none
091208B	10265	10263	-	-	-
100111A	10317	none	none	none	none
100115A	10325	none	none	none	none
100213B	10412	10422	-	-	-
100316A	10501	none	none	none	none
100316B	10500	10495	-	-	-
100423A	10651	none	none	none	10658
100514A	10761	none	none	none	none
100702A	10926	none	none	none	none
100704A	10929	none	none	10940	-
100727A	11001	none	none	none	none
100802A	11031	none	none	none	none
100814A	11094	11089	-	-	-
100823A	11135	none	none	none	none
100917A	11289	none	none	none	none
101008A	11318	none	none	none	11318
101011A	11332	none	none	none	11331
101017A	11345	none	none	none	11345
101023A	11363	none	none	none	none
101114A	11405	none	none	none	none
101213A	11448	11457	-	-	-
110102A	11509	none	none	none	none

GRB#	F.R.E.D.	Redshift	”High-z”	Any z	Peaks
110223A	11764	none	none	none	none
Total:	111	77	71	59	49

Table 4. GRBs of the samples used for this study and the GCN used to discriminate each burst.